THYROID
Volume 25, Number 6, 2015

DOI: 10.1089/thy.2014.0419

Using Diffusion-Weighted MRI to Predict Aggressive Histological Features in Papillary Thyroid Carcinoma: A Novel Tool for Pre-Operative Risk Stratification in Thyroid Cancer

Yonggang Lu,[1] Andre L. Moreira,[2] Vaios Hatzoglou,[3] Hilda E. Stambuk,[3] Mithat Gonen,[4] Yousef Mazaheri,[1,3] Joseph O. Deasy,[1] Ashok R. Shaha,[5] R. Michael Tuttle,[6] and Amita Shukla-Dave[1,3]

Background: Initial management recommendations of papillary thyroid carcinoma (PTC) are very dependent on preoperative studies designed to evaluate the presence of PTC with aggressive features. The purpose of this study was to evaluate whether diffusion-weighted magnetic resonance imaging (DW-MRI) before surgery can be used as a tool to stratify tumor aggressiveness in patients with PTC.
Methods: In this prospective study, 28 patients with PTC underwent DW-MRI studies on a three Tesla MR scanner prior to thyroidectomy. Due to image quality, 21 patients were finally suitable for further analysis. Apparent diffusion coefficients (ADCs) of normal thyroid tissues and PTCs for 21 patients were calculated. Tumor aggressiveness was defined by surgical histopathology. The Mann-Whitney U test was used to compare the difference in ADCs among groups of normal thyroid tissues and PTCs with and without features of tumor aggressiveness. Receiver operating characteristic (ROC) analysis was performed to assess the discriminative specificity, sensitivity, and accuracy of and determine the cutoff value for the ADC in stratifying PTCs with tumor aggressiveness.
Results: There was no significant difference in ADC values between normal thyroid tissues and PTCs. However, ADC values of PTCs with extrathyroidal extension (ETE; $1.53 \pm 0.25 \times 10^{-3}$ mm^2/s) were significantly lower than corresponding values from PTCs without ETE ($2.37 \pm 0.67 \times 10^{-3}$ mm^2/s; $p < 0.005$). ADC values identified 3 papillary carcinoma patients with extrathyroidal extension that would have otherwise been candidates for observation based on ultrasound evaluations. The cutoff value of ADC to discriminate PTCs with and without ETE was determined at 1.85×10^{-3} mm^2/s with a sensitivity of 85%, specificity of 85%, and ROC curve area of 0.85.
Conclusion: ADC value derived from DW-MRI before surgery has the potential to stratify ETE in patients with PTCs.

Introduction

Patients with intrathyroidal, well-differentiated papillary thyroid carcinoma (PTC) have relatively low-risk malignant tumors with a recurrence rate of 3% to 4% or lower and a disease-specific survival rate of more than 99% (1). Traditionally, the initial treatment of PTC has included a total thyroidectomy, often with radioactive iodine remnant ablation (2). However, a more risk adapted management approach has been followed at many centers (3,4) and is now being endorsed in both the National Comprehensive Cancer Center and the American Thyroid Association guidelines (5,6). Furthermore, very low risk thyroid cancer patients with intrathyroidal papillary microcarcinoma may not even require thyroid surgery, as they can be safely followed with an active surveillance management approach (7). Therefore, initial management recommendations are very dependent on preoperative studies designed to evaluate the presence of PTC with aggressive features such as extrathyroidal extension, locoregional metastases, or distant metastases.

While fine-needle aspiration (FNA) cytology is the most widely used method for preoperative evaluation of thyroid nodules (8), it provides only minimal information with regard to tumor aggressiveness (9). Currently, tumor aggressiveness is based on surgical histological analysis, which is only available after surgical resection of the thyroid gland (10). While commonly used as the primary imaging modality for thyroid, thyroid nodules, and cervical lymph nodes, routine neck ultrasonography cannot reliably exclude minor extrathyroidal extension (11,12). This has significant clinical implications since the presence of extrathyroidal extension is a marker of a potentially more aggressive tumor behavior that

Departments of [1]Medical Physics, [2]Pathology, [3]Radiology, [4] Epidemiology and Biostatistics, [5]Surgery, and [6]Medicine, Memorial Sloan-Kettering Cancer Center, New York, New York.

would lead to more aggressive initial therapy (likely total thyroidectomy and perhaps radioactive iodine ablation). This is particularly important in the evaluation of papillary thyroid microcarcinomas that are being considered for an active surveillance observational management approach (13). Therefore, there remains a pressing need for noninvasive tests to identify patients with histologically aggressive tumors so that patients unlikely to have aggressive tumors can be observed or treated with less than a total thyroidectomy and radioactive iodine ablation.

Diffusion-weighted magnetic resonance imaging (DW-MRI) allows for quantitative and non-invasive measurement of the Brownian motion of water molecules. Use of DW-MRI as a surrogate marker to probe tumor aggressiveness is compelling, because this measurement is strongly affected by changes in tissue organization at the cellular level (14). These microstructural changes affect the motion of water molecules and alter water diffusion properties and DW-MRI signal intensity. The loss of signal intensity in DW-MRI can be quantified by measuring the apparent diffusion coefficient (ADC), which is the indicator of water molecular motion that is affected by cellular organization (14). Recently, ADC value has shown potential as a surrogate imaging biomarker to assess tumor aggressiveness in breast (15), prostate (16–18), and rectal cancers (19). For thyroid cancers, DW-MRI has been applied in the assessment of thyroid nodules, especially for the differentiation of benign and malignant tumors (20–27). The purpose of this study was to evaluate whether ADC calculated from DW-MRI data before surgery stratifies tumor aggressiveness as defined at surgical histopathology analysis in PTCs.

Materials and Methods

Patients

Between January 2011 and March 2012, all adult patients (≥ 18 years) undergoing surgical consultation for thyroidectomy on the basis of a thyroid nodule FNA demonstrating either papillary thyroid cancer or suspicious for thyroid cancer in our institution were offered enrollment in a prospective clinical trial evaluating multiparametric MRI including DW-MRI in head and neck tumors. This prospective protocol was approved by our local institutional review board. After providing appropriate informed consent, 28 subjects underwent the research MRI prior to thyroid surgery. The exclusion criteria were: (i) presence of contraindication to MRI, (ii) tumor size larger than 5 cm (detected by ultrasonography), and (iii) patients who are claustrophobic.

MRI study

MRI examination was performed on a 3-Tesla GE scanner (General Electric, Milwaukee, WI) using an eight-channel neurovascular phased-array coil. The MRI study consisted of standard multiplanar (sagittal, axial, coronal) T1- and T2-weighted imaging scans followed by DW-MRI scans. A T1 weighted image relies upon the longitudinal relaxation of a tissue's net magnetisation vector and a T2 weighted image reflects the transverse relaxation of the net magnetisation vector with respect to the external magnetic field. The duration of the whole examination was approximately 30 minutes.

The T1- and T2-weighted MRI scans covered the whole thyroid gland with a slice thickness of 5 mm, field of view (FOV) of 20–24 cm, and acquisition matrix of 256×256. For T1-weighted MRI, TR (repetition time) = 500 ms, and TE (echo time) = 15 ms; for T2-weighted MRI, TR = 4000 ms, and TE = 80 ms.

DW-MRI data were acquired using a single-shot echo planar imaging (SS-EPI) spin echo sequence (TR = 4000 ms; TE = 98–104 ms; number of excitation = 4; three orthogonal directions) with b value of 500 s/mm^2). The b value was chosen after assessing DW-MR image quality and reviewing the literature (24). Fat-suppression, shimming (shimming FOV = $14 \sim 16$ cm), and parallel imaging (acceleration factor = 2) techniques were used. The DW-MRI scans were focused on thyroid tumors with 4 to 8 slices of 5-mm thickness, 0-mm gap, $20 \sim 24$-cm FOV, and 128×128 acquisition matrix, which was zero-filled and reconstructed to 256×256 pixels. Before scanning, a calibration scan was used to reduce Nyquist (N/2) ghosting artifacts. Images were all obtained in axial planes.

The regions of interest (ROIs) for PTC were placed on thyroid glands avoiding obvious cystic, hemorrhagic, or calcified portions. The ROI for normal thyroid tissue was placed on the selected one slice of whole lobe contralateral to the PTC. The ROIs were drawn on the DW-MR images by a neuroradiologist with more than 10 years of experience based on the radiological and clinical information including ultrasound reports. The ROI encompassed the entire nodule of interest with a minimum ROI considered to be 0.1 cm^3 (i.e., 17 voxels). A single ROI was used for normal tissue analysis while the mean ADC of the ROI was used when multiple nodules were evaluated.

The ADC value for each ROI was calculated using a mono-exponential model: $S/S_0 = \exp(-b \times \mathrm{ADC})$, where S and S_0 are the signal intensities with and without diffusion weighting, respectively, and b is the gradient factor (b value, s/mm^2). ADC was then calculated as $-\ln(S/S_0)/b$. A noise floor rectification scheme was used in the ADC calculation (28), which was performed on a voxel-by-voxel basis, generating an ADC map as well as averaged values for the ROIs. In order to suppress the technical factors influencing the ADC values, a normalized ADC value (nADC) was calculated (the ratio of ADC value of PTCs to the ADC value of normal thyroid tissue).

Before the patient study, a DW-MRI study with the ice-water phantom was performed to evaluate repeatability of the ADC measurement. The MRI study of the phantom consisted of four repeat scans with the same settings as the MRI studies of the patients. The phantom consisted of a 3.8-liter plastic container with a single, sealed, 175-mL measurement tube prefilled with distilled water. Prior to taking the MRI scans, crushed ice and water were added such that the ice water filled the entire volume of the container. After a thermal equilibrium between the water in the tube and the surrounding ice bath was reached, the phantom was delivered to the MRI room for scanning.

In order to evaluate the repeatability of ADC measurement in human thyroid glands, data from 9 healthy volunteers (age, 23–50 years; male:female, 4:5) were analyzed for another DW-MRI study, which consisted of three longitudinal exams (2 weeks apart) for each subject with an identical MRI protocol. The study was also approved by the local institutional review board, and all volunteers were provided written informed consents. ADC values was calculated from a fixed circle area (8-mm diameter) placed on the thyroid gland of

human subject. The within-subject coefficient of variation (wCV) was calculated to assess the repeatability of the ADC measurement by using the Quantitative Imaging Biomarker Alliance (Radiological Society of North America) proposed statistical metrics (29,30): $wCV = \sigma_w/\mu$, where μ is the overall mean of ADC measurement and, σ_w is the standard deviation of ADC measurements within subject.

Histopathologic examination

Surgical specimens of the thyroid tumors taken after radical thyroidectomy or lobectomy were collected under the supervision of a pathologist with more than 10 years of experience. Paraffin-embedded tissue blocks were obtained for each surgically resected specimen by sectioning each tumor. The section of each thyroid tumor was stained with hematoxylin and eosin. The pathologist reviewed the hematoxylin and eosin section of each thyroid tumor and used established criteria to evaluate tumor aggressiveness (31,32). Tumor aggressiveness was evaluated individually using the following six histopathologic features: tall cell variants, necrosis, vascular and/or tumor capsular invasion, extrathyroidal extension, regional metastases, and distant metastases. A tumor with presence of any one of these features was regarded to be aggressive.

Statistical analysis

A nonparametric Mann-Whitney U test with Bonferroni correction for multiple testing was used to compare the parametric differences among groups of normal thyroid tissues, PTCs, and PTCs with and without features of tumor aggressiveness (six features mentioned above). The receiver operating characteristic (ROC) curve constructed from the probability of logistic regression analysis was used to assess the discriminative specificity, sensitivity, and accuracy between PTCs with and without features of tumor aggressiveness. The cutoff value of the ADC (nADC) for stratifying tumor aggressiveness was also determined based on the criteria of maximum area under the ROC curve. A *p*-value of less than 0.05 was considered to indicate statistical significance.

All data analysis was performed by an in-house software using Matlab R2008a on a Microsoft Windows system.

Table 1. Patient Characteristics of the 21 Patients with Magnetic Resonance Imaging Studies Suitable for Analyses

Characteristic	n *(%)*
Age at diagnosis (years)	
21 evaluable patients	39 ± 7 years (range 26–49 years)
Sex	
Female	18 (85%)
Male	3 (15%)
Fine-needle aspiration cytology	
Papillary thyroid cancer	16 (76%)
Suspicious for papillary thyroid cancer	5 (24%)
Preoperative ultrasound	
Subcapsular location of tumor	16 (76%)
Extrathyroidal extension	None
Evidence of lymph node metastases	7 (33%)
Histology	
Classic papillary thyroid cancer	12 (57%)
Follicular variant papillary thyroid cancer	3 (14%)
Tall cell variant papillary thyroid cancer	6 (29%)
Extrathyroidal extension by histology	7 (33%)
Vascular invasion by histology	1 (5%)
Size of papillary thyroid carcinoma	14.5 ± 6.7 mm (0.5–25 mm)
Pathology T	
T1a (papillary microcarcinoma)	5 (24%)
T1b	13 (62%)
T2	3 (14%)
Pathology N	
N0	9 (43%)
N1	12 (57%)
Clinical M	
M0	21
M1	None
AJCC Stage	
1	19 (90%)
3	2 (10%)

T, N and M are categories within the AJCC (American Joint Committee on Cancer) staging system.

Results

Of the 28 patients enrolled in the study, 7 patients were excluded from the study due to either distorted image quality ($n = 5$) or because the tumor was too small to see on DWI images ($n = 2$). Clinicopathological features of the 21 patients (mean age 39 ± 7 years at diagnosis, 85% female) included in the final analysis are presented in Table 1. None of the patients had extrathyroidal extension (ETE) identified on the preoperative ultrasound examination. Of the 21 patients, 7 patients were found to have locoregional metastases by preoperative ultrasound imaging the remaining 14 patients had no preoperative ultrasonographic evidence of aggressive disease. Thyroid nodule FNA demonstrated 16 patients with cytology consistent with papillary thyroid cancer (Bethesda VI) and 5 suspicious for thyroid cancer (Bethesda V). Based on surgical pathology analysis, all 21 patients had PTCs [12 classic PTC, 3 follicular variant PTC, and 6 with the tall cell features/variant, 1 patient with vascular and/or capsular invasion, 7 patients with ETE, and 12 patients with locoregional metastases (pN1)]. The mean maximum size of the lesion was 14.5 ± 6.7 mm and ranged from 0.5 to 25 mm (with the papillary microcarcinomas being 0.5, 3, 8, 8 and 10 mm). From the DW-MR images, the volumes of the patients' tumors ranged from 0.1 cm^3 to 5 cm^3 (there were 12 tumors $< 1\ cm^3$, 8 tumors of 1–4 cm^3, and 1 tumor $> 4\ cm^3$).

The ADC values of water calculated from the ROI (as seen in Fig. 1) in the ice-water phantom at four repeat scans were 1.113, 1.112, 1.113, and 1.112×10^{-3} mm^2/s, respectively. These ADC values were consistent with the literature (33,34), showing that the ADC measurement was highly reproducible in DW-MRI. In another study with healthy volunteers, the ADC values of thyroid gland from 9 volunteers across the exams were 1.84 ± 0.33 vs 1.74 ± 0.27 vs 1.74 ±

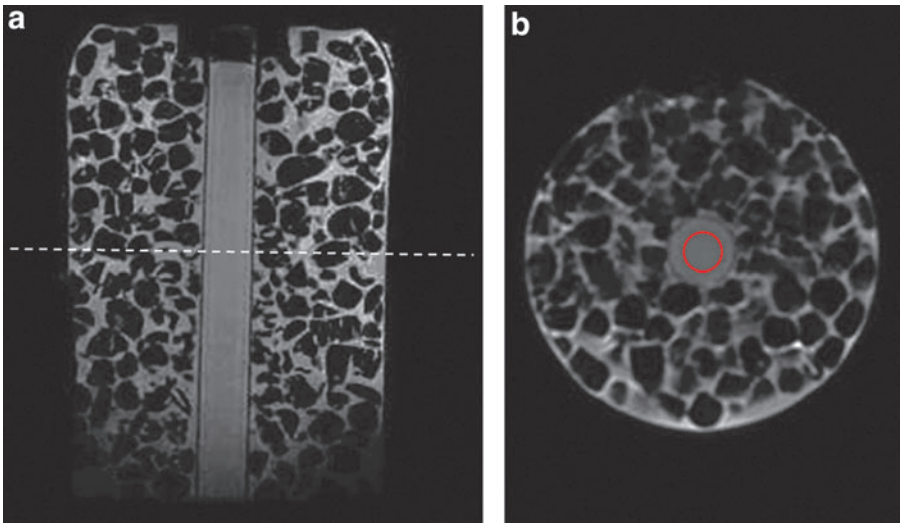

FIG. 1. Magnetic resonance (MR) images for an ice-water phantom. **(a)** A sagittal T1-weighted image. **(b)** A slice of axial diffusion-weighted MR (DW-MR) image ($\mathbf{b} = 500\ s/mm^2$) at the location shown in **a** as a dashed line. The region of interest for calculating the apparent diffusion coefficient (ADC) is shown with a red circle.

0.23×10^{-3} mm^2/s, respectively. There is no significant difference in ADC values among the three longitudinal exams. The calculated within-subject coefficient of variation (wCV) of ADC values was 10.33%, showing a high repeatability of ADC measurement in DW-MRI.

The ADC values for normal thyroid tissues from the 21 patients were $1.91 \pm 0.38 \times 10^{-3}$ mm^2/s (mean ± standard deviation), the ADC (nADC) values for 21 PTCs were $2.09 \pm 0.69 \times 10^{-3}$ mm^2/s (0.96 ± 0.26). No significant difference was found in ADC (nADC) values between normal thyroid tissues and PTCs ($p = 0.48$ (0.16)).

Among the six tumor aggressive features, extrathyroidal extension (ETE) was the only feature found to be significant in its ability to stratify PTCs: The ADC (nADC) values of PTCs with ETE ($1.53 \pm 0.25 \times 10^{-3}$ mm^2/s (0.77 ± 0.14)) were significantly lower than corresponding ADC values from PTCs without ETE ($2.37 \pm 0.67 \times 10^{-3}$ mm^2/s (1.28 ± 0.33); $p < 0.005$ ($p < 0.0003$)), as shown in Figures 2a and b. The no-ETE group consisted of all PTCs without histological evidence of extrathyroidal extension. Additionally, the ADC (nADC) values of normal thyroid tissue [$1.91 \pm 0.38 \times 10^{-3}$ mm^2/s (1)] were significantly lower than corresponding ADC (nADC) values from PTCs without ETE [$2.37 \pm 0.67 \times 10^{-3}$ mm^2/s (1.28 ± 0.33); $p < 0.01$ ($p < 0.001$)], and higher than corresponding ADC values from PTCs with ETE [$1.53 \pm 0.25 \times 10^{-3}$ mm^2/s (0.77 ± 0.14); $p < 0.01$ ($p < 0.001$)]. By using ROC analysis, the cutoff value of ADC (nADC) that discriminates between PTCs with and without ETE was determined [ADC = 1.85×10^{-3} mm^2/s (0.9532)] with a sensitivity of 85% (100%), specificity of 85% (100%), and ROC curve area of 0.85 (1.00) (Fig. 3). From the derived ADC cutoff value, 3 PTC patients were identified with extrathyroidal extension that would have otherwise been candidates for observation based on ultrasound evaluations (no evidence of locoregional metastases or extrathyroidal extension was evident on preoperative ultrasound imaging).

Figure 4 shows typical images from a representative PTC patient with ETE verified by pathological analysis. Images from pathological analysis demonstrated that papillae were lined by cells with columnar shape (a feature of tall cell variants; see Fig. 4e) and tumor extended into surrounding fibroadipose tissue (see Fig. 4f), clearly showing a histologically more aggressive tumor. The ADC value for the PTC with ETE was lower than that for normal thyroid tissue ($1.65 \pm 0.18 \times 10^{-3}$ mm^2/s vs. $2.45 \pm 0.22 \times 10^{-3}$ mm^2/s).

Images from a representative PTC without ETE seen on pathological analysis is shown in Figure 5. Figures 5e and f demonstrate a classical papillary carcinoma that was

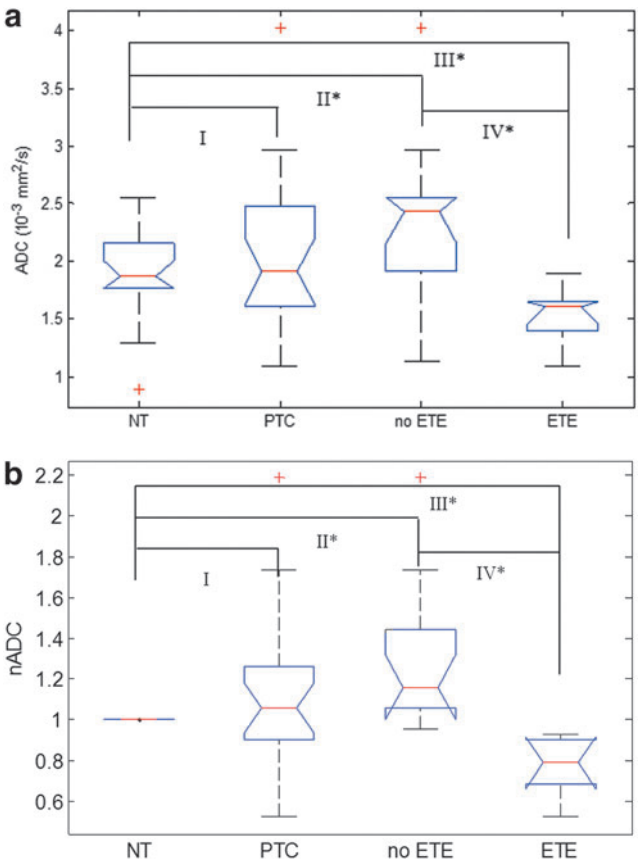

FIG. 2. Box-and-whisker plots demonstrating changes in ADC **(a)** and nADC **(b)** values between the normal thyroid tissues (NT), papillary thyroid carcinomas (PTCs), PTCs without extrathyroidal extension (no ETE), and PTCs with extrathyroidal extension (ETE). Asterisks (*) denote significance ($p < 0.05$) between different tissue types (II: NT and no-ETE; III: NT and ETE; IV: ETE and no-ETE). The red crosses (+) delineate outliers in the data set.

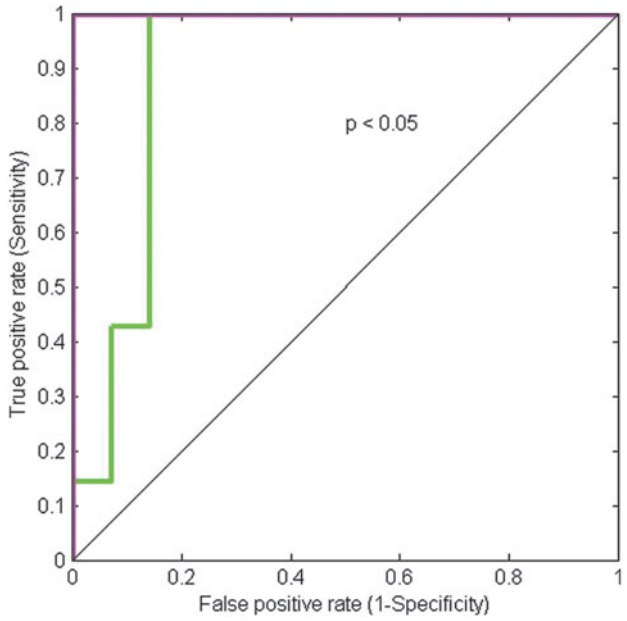

FIG. 3. ROC curve to discriminate PTCs with and without features of ETE using ADC (the green curve) and nADC (the magenta curve).

confined by the capsule and papillae that are lined up by neoplastic cells, showing classical nuclear features such as open and clear chromatin. The ADC value for this PTC without ETE was higher than that for normal thyroid tissue ($2.34 \pm 0.53 \times 10^{-3}$ mm^2/s vs. $2.25 \pm 0.52 \times 10^{-3}$ mm^2/s).

Of 21 PTCs, there were 5 microcarcinomas (0.5–10 mm), all of which had no ETE and no evidence of locoregional or distant metastases based on histological analysis. Four of the five microcarcinomas were in a subcapsular location without evidence of extrathyroidal extension. By using ADC values, no significance was found between PTCs with and without microcarcinoma ($2.11 \pm 0.90 \times 10^{-3}$ mm^2/s vs. $1.82 \pm 0.53 \times 10^{-3}$ mm^2/s, $p = 0.33$). However, by using nADC, there was a significance found: nADCs from PTCs with microcarcinoma were significantly higher than that from PTCs without microcarcinoma (1.25 ± 0.27 vs. 0.87 ± 0.29, $p = 0.02$). Figure 6 shows a histological image in a microcarcinoma with the tumor size of 10 mm (on pathology), which is a follicular variant of papillary carcinoma. In this microphotograph, nuclear features of papillary carcinoma (nuclear grooves and clear chromatin pattern) can be seen. The ADC value for this microcarcinoma was 2.63×10^{-3} mm^2/s.

Discussion

Noninvasive assessment of tumor aggressiveness in PTCs before surgery has the potential to dramatically improve

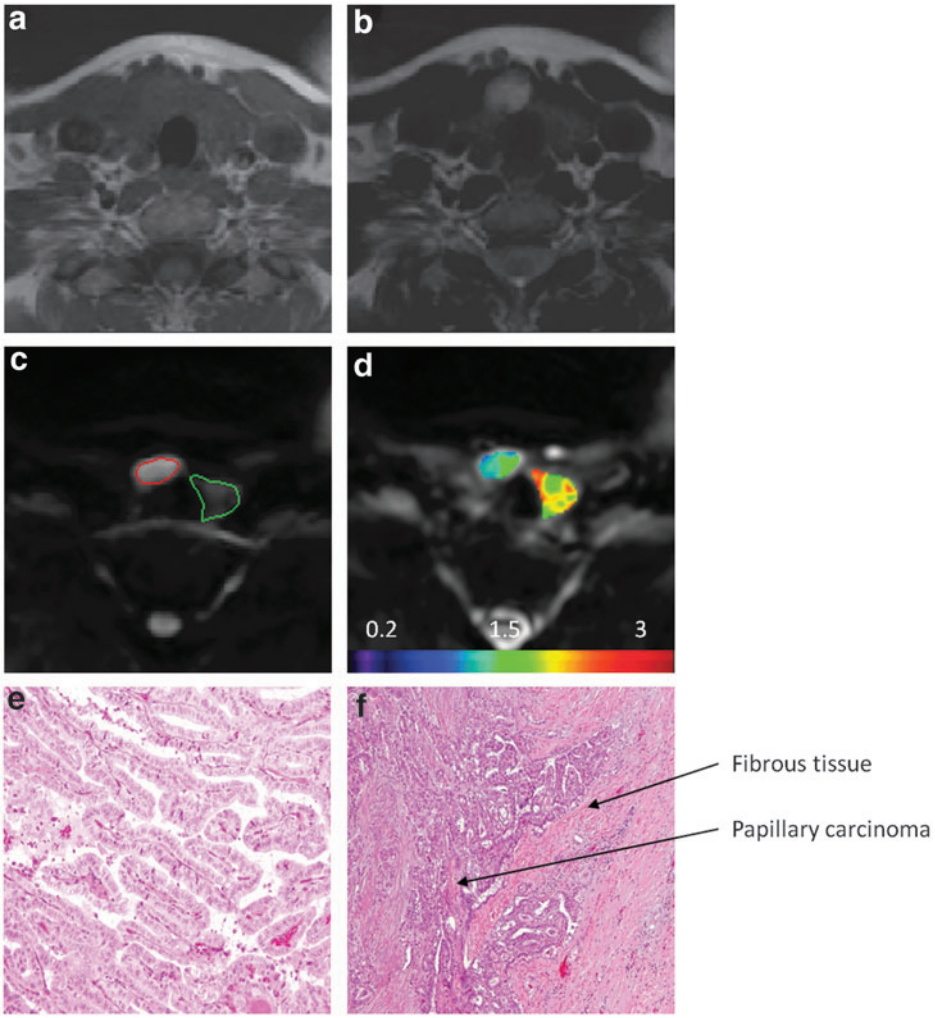

FIG. 4. Images from a representative PTC patient with ETE (female, 47 years old). **(a)** T1-weighted MR image. **(b)** T2-weighted MR image. **(c)** DW-MR image (**b** = 500 s/mm^2). The area outlined in red is the region of PTC, and the area outlined in green is the region with normal thyroid tissue. **(d)** ADC map overlaid on DW-MR image (**b** = 0 s/mm^2). **(e)** Histopathological hematoxylin and eosin (H&E) image of a PTC with features of a tall cell variant (total magnification, 10×). **(f)** Histopathological H&E image of a PTC showing ETE (total magnification, 4×). The ADC value for the PTC (tumor size on pathology was 25 mm) was lower than that for normal thyroid tissue ($1.65 \pm 0.18 \times 10^{-3}$ mm^2/s vs. $2.45 \pm 0.22 \times 10^{-3}$ mm^2/s).

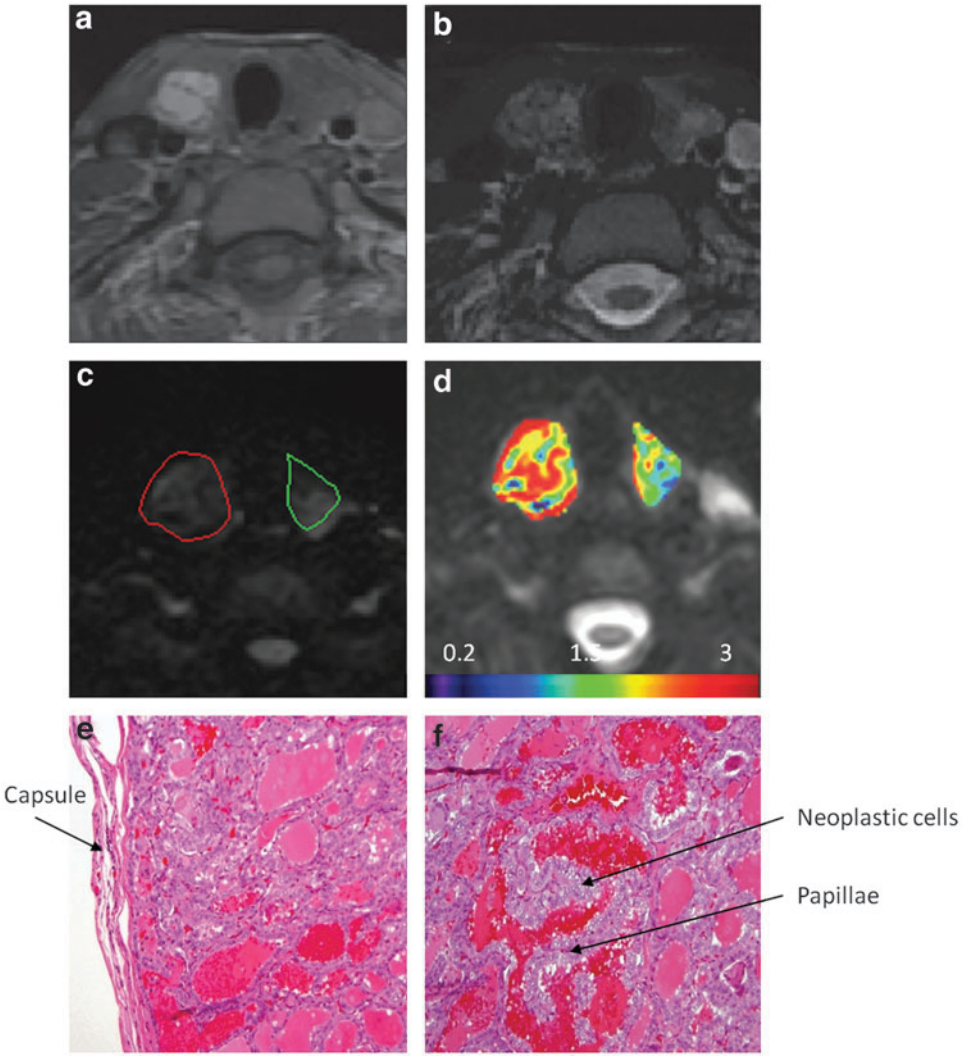

FIG. 5. Images from a representative patient without ETE (female, 34 years old). **(a)** A T1-weighted MR image. **(b)** A T2-weighted MR image. **(c)** A DW-MR image ($\mathbf{b} = 500\ s/mm^2$). The area outlined in red is the region of PTC, and the area outlined in green is the region with normal thyroid tissue. **(d)** ADC map overlaid on DW-MR image ($b = 0\ s/mm^2$). **(e)** Histopathological H&E image of a classical PTC (total magnification, 10×). **(f)** Histopathological H&E image of a classical PTC (total magnification, 20×). The ADC value for the PTC (tumor size on pathology was 20 mm) was higher than that for normal thyroid tissue ($2.34 \pm 0.53 \times 10^{-3}$ mm^2/s vs. $2.25 \pm 0.52 \times 10^{-3}$ mm^2/s).

preoperative risk stratification in PTC patients. The preliminary results in this prospective pilot study indicate that ADC values derived from DW-MRI data have the potential to stratify PTCs based on ETE. The findings show that PTCs with ETE had significantly lower ADC values than those without ETE ($1.53 \pm 0.25 \times 10^{-3}$ mm^2/s vs. $2.37 \pm 0.67 \times 10^{-3}$ mm^2/s; $p < 0.005$). The cutoff value of ADC to stratify PTCs into tumor groups with and without ETE was 1.85×10^{-3} mm^2/s.

In the present study, we correlated ADC values with different features of tumor aggressiveness. Only the ETE feature

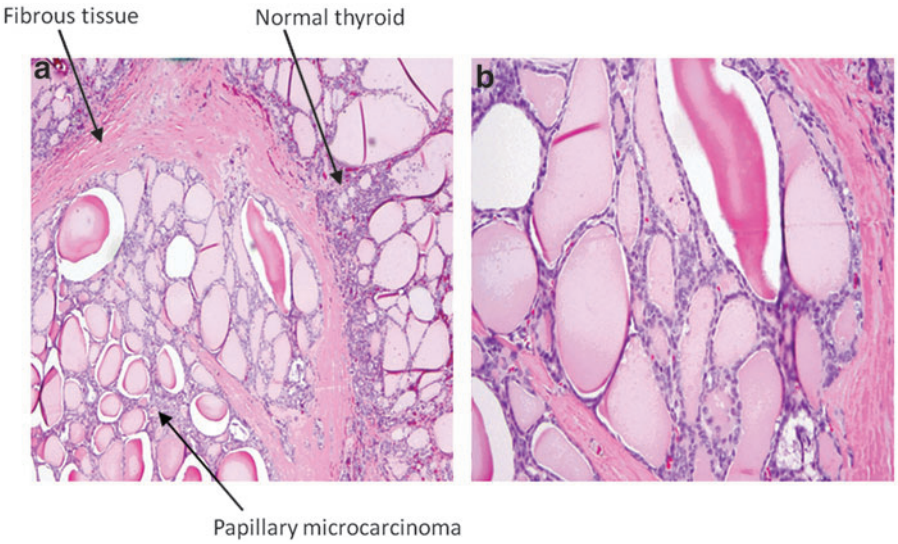

FIG. 6. Histopathological H&E images of a papillary microcarcinoma (note the paler staining pattern of neoplastic cells) at **(a)** a total magnification of 40× and **(b)** a total magnification of 100×.

was found to be significant. ETE is defined as extension of the primary tumor outside of the thyroid capsule with invasion into the surrounding structures (35). Gross ETE has been identified as carrying a higher risk for local recurrence (36,37) and is used in several staging systems, including TNM (tumor, node, and metastasis) (38), AGES (age, grade, ETE, and size) (39), AMES (age, metastasis, ETE, and size) (40), and MACIS (metastasis, age, completeness of resection, invasion, and size) (41). Since an active surveillance management approach or an initial surgery less than a total thyroidectomy are best reserved for patients with intrathyroidal PTC, the ability to predict the presence of ETE using diffusion weighted MRI will allow the clinician to identify patients that are likely to benefit from more aggressive initial therapy and therefore have a significant impact on clinical management, particularly in low risk thyroid cancers.

In general, tumors with higher degrees of aggressiveness are characterized by increased cell attenuation, enlarged nuclei, hyperchromatism, and more barriers to diffusion (42). These histopathological characteristics reduce the extracellular dimension that leads to a decrease in ADC values. Although there is no similar study in thyroid cancers, our results are consistent with studies that evaluated tumor aggressiveness in other types of cancers, such as prostate and rectal cancers. For example, Oto *et al*. revealed that in prostate cancer, ADC values showed a negative correlation with Gleason score (16), In prostate cancer higher Gleason score tumors are more aggressive. Curvo-Semedo *et al*. also found that in rectal cancer, there was a significant negative correlation between ADC values and the tumor differentiation grade at histology (19). Lawrence *et al*. showed that the ADC parameters of median and 10th and 25th percentiles had a statistically significant difference between tumors with and those without extracapsular extension (ECE) ($p < 0.05$)(43). Chong *et al*. also found that the mean tumor ADC values were significantly lower in prostate cancer patients with ECE than patients without ECE ($p < 0.001$) (44). Therefore, DW-MRI has begun to show its utility in assessing site-specific risk of extracapsular extension in prostate cancers.

Razek *et al*. reported that malignant thyroid nodules had lower ADC values than benign thyroid nodules (24). It differs from the present study as they had a mixed patient population that included both PTCs and follicular carcinomas and the study was carried out at 1.5T MRI. In our study it is interesting to notice that no significant difference was found between normal thyroid tissues and PTCs and even more interesting that PTCs without aggressive features had significantly higher ADC values than normal thyroid tissues. A possible explanation is that PTCs without aggressive features have greater number and size of colloid filled spaces than normal thyroid tissues. The abundant extracellular fluid leads to an increased capacity for water diffusion and therefore, increased ADC values. Comparatively, normal thyroid tissue has only small follicles, usually filled with colloid depending on the functional activity of the gland. The diffusion capacity in normal thyroid tissue is influenced by high cell attenuation, which results in restricted motion of water molecules and low ADC values. Schueller *et al*. also found similar results with thyroid carcinomas, for which the ADC values ($2.43–3.037 \times 10^{-3}$ mm^2/s) were significantly higher than those for normal thyroid tissue ($1.253–1.602 \times 10^{-3}$ mm^2/s) (25). Another consideration is that our sample size was too small to accurately evaluate the impact of the other high risk features such as vascular invasion and distant metastases. DW-MRI data acquired with an EPI sequence has inherent drawbacks, such as susceptibility, chemical shift, and Nyquist (N/2) ghosting artifacts. In our study, we took several strategies to reduce these artifacts by using parallel imaging, fat suppression, calibration scan, and shimming. Another important issue when acquiring the DW-MRI data was the *b* value setting. Data acquired at high *b* value can more exclusively reflect the effect of diffusion but could exacerbate the artifacts. Data acquired at low *b* value ($< 200\ s/mm^2$) has relatively better image quality than data acquired at high *b* value but could be influenced by perfusion. The *b* value of $500\ s/mm^2$ was used in our study to acquire DW-MR images with sufficient diffusion weighting and image quality. The *b* values used by other investigators (24,25,27,45) were in the range of $128 \sim 1000\ s/mm^2$.

From a clinical perspective, this pilot study suggests that DW-MRI could have clinical relevance in providing additional risk stratification information for small thyroid cancers that appear to be confined to the thyroid based on standard preoperative ultrasound and clinical evaluations. For example, the ADC value identified three papillary carcinomas with minor extrathyroidal extension that would have otherwise been acceptable candidates for an observational management approach. From a technical standpoint, multiparametric MRI including DW-MRI can be performed in 30 minutes or less using standard MRI equipment with appropriate region of interest and statistical analyses. If these observations are validated in larger prospective trials, it is likely that DW-MRI could provide information that could augment the standard preoperative ultrasound evaluation when patients are being considered for an observational management approach rather than immediate surgical resection.

The purpose of this study was to evaluate whether DW-MRI before surgery can be used as a potential routine tool to stratify patients with PTC into two groups—one group has aggressive tumor features waiting for surgery, and another group has no aggressive tumor features—who are suitable candidates for active surveillance. MRI is a noninvasive imaging method with advantages of anatomical and functional characterization without any ionizing radiation. With advancement of technique, MRI is currently commonly available in many institutions worldwide with easy and fast clinical setup. Therefore, MRI may be a good option for PTC patients being considered for active surveillance treatment approach.

There are a few limitations in this study. Firstly, this study is a feasibility study and thereby has a small number of PTC patients. A larger cohort of patients is necessary to confirm our initial findings. Secondly, SS-EPI–based DW-MRI data suffers from susceptibility artifacts at the region of the head and neck, especially at high magnetic field (3T). Alternative techniques, such as multiple-shot fast spin echo DW-MRI (46) and DW-MRI with line scan data acquisition (47), can reduce this artifact. However, clinically, SS-EPI–based DW-MRI is the most commonly used technique worldwide (42). Finally, we do not have clinical or follow up data on the potentially eligible subjects that chose not to participate and therefore cannot exclude an unknown selection bias that could have influenced our results.

In conclusion, this study demonstrates that ADC values derived from DW-MRI before surgery have the potential to stratify patients based on ETE in PTCs. The experimental results show that there was a significant tendency toward lower ADC values in PTCs with ETE. The results suggest that ADC may be a surrogate imaging biomarker that can guide critical initial management recommendations for patients with PTCs.

Acknowledgments

The authors would like to thank the MRI technologists for their great efforts to help perform all examinations and Mr. Christian Czmielewski (MSc) for his kind contribution to data management. Thanks also are given to Ms. Sandhya George (BA) for carefully editing the manuscript. We would especially like to show our appreciation for Dr. Thomas L. Chenevert from the University of Michigan for generously providing us with the ice-water phantom and detailed guidelines.

This research was supported by the National Cancer Institute/National Institutes of Health (grant numbers R21CA176660-01A1 and P50 CA172012-01A1).

Author Disclosure Statement

The authors hereby state that none of authors have any conflict of interest.

References

1. Hay ID 2007 Management of patients with low-risk papillary thyroid carcinoma. Endocr Pract **13:**521–533.
2. Vaisman F, Momesso D, Bulzico DA, Pessoa CH, da Cruz MD, Dias F, Corbo R, Vaisman M, Tuttle RM 2013 Thyroid lobectomy is associated with excellent clinical outcomes in properly selected differentiated thyroid cancer patients with primary tumors greater than 1 cm. J Thyroid Res **2013:**398194.
3. Tuttle RM, Sabra MM 2013 Selective use of RAI for ablation and adjuvant therapy after total thyroidectomy for differentiated thyroid cancer: a practical approach to clinical decision making. Oral Oncol **49:**676–683.
4. Tuttle RM 2008 Risk-adapted management of thyroid cancer. Endocr Pract **14:**764–774.
5. National Comprehensive Cancer Network 2014 Guidelines for treatment of cancer by site: thyroid carcinoma. Available at www.nccn.org/professionals/physician_gls/f_guidelines.asp#site (accessed February 15, 2015).
6. American Thyroid Association (ATA) 2014 Guidelines on Thyroid Nodules and Differentiated Thyroid Cancer—Highlights, Consensus, and Controversies. ATA Satellite Symposium, June 20, 2014, Chicago, Illinois. www.thyroid.org/webcast-and-enduring-cme-for-the-june-20–2014-ata-program-is-available (accessed February 15, 2015).
7. Ito Y, Higashiyama T, Takamura Y, Kobayashi K, Miya A, Miyauchi A 2010 Clinical outcomes of patients with papillary thyroid carcinoma after the detection of distant recurrence. World J Surg **34:**2333–2337.
8. Cooper DS, Doherty GM, Haugen BR, Kloos RT, Lee SL, Mandel SJ, Mazzaferri EL, McIver B, Pacini F, Schlumberger M, Sherman SI, Steward DL, Tuttle RM 2009 Revised American Thyroid Association management guidelines for patients with thyroid nodules and differentiated thyroid cancer. Thyroid **19:**1167–1214.
9. Baloch ZW, LiVolsi VA, Asa SL, Rosai J, Merino MJ, Randolph G, Vielh P, DeMay RM, Sidawy MK, Frable WJ 2008 Diagnostic terminology and morphologic criteria for cytologic diagnosis of thyroid lesions: a synopsis of the National Cancer Institute Thyroid Fine-Needle Aspiration State of the Science Conference. Diagn Cytopathol **36:**425–437.
10. Miller B, Burkey S, Lindberg G, Snyder WH, 3rd, Nwariaku FE 2004 Prevalence of malignancy within cytologically indeterminate thyroid nodules. Am J Surg **188:**459–462.
11. Lee CY, Kim SJ, Ko KR, Chung KW, Lee JH 2014 Predictive factors for extrathyroidal extension of papillary thyroid carcinoma based on preoperative sonography. J Ultrasound Med **33:**231–238.
12. Gweon HM, Son EJ, Youk JH, Kim JA, Park CS 2014 Preoperative assessment of extrathyroidal extension of papillary thyroid carcinoma: comparison of 2- and 3-dimensional sonography. J Ultrasound Med **33:**819–825.
13. Moon SJ, Kim DW, Kim SJ, Ha TK, Park HK, Jung SJ 2014 Ultrasound assesment of degrees of extrathyroidal extension in papillart thyroid microcarcinoma. Endocr Pract **20:**1–25.
14. Le Bihan D, Turner R, Douek P, Patronas N 1992 Diffusion MR imaging: clinical applications. AJR Am J Roentgenol **159:**591–599.
15. Costantini M, Belli P, Rinaldi P, Bufi E, Giardina G, Franceschini G, Petrone G, Bonomo L 2010 Diffusion-weighted imaging in breast cancer: relationship between apparent diffusion coefficient and tumour aggressiveness. Clin Radiol **65:**1005–1012.
16. Oto A, Yang C, Kayhan A, Tretiakova M, Antic T, Schmid-Tannwald C, Eggener S, Karczmar GS, Stadler WM 2011 Diffusion-weighted and dynamic contrast-enhanced MRI of prostate cancer: correlation of quantitative MR parameters with Gleason score and tumor angiogenesis. AJR Am J Roentgenol **197:**1382–1390.
17. Vargas HA, Akin O, Franiel T, Mazaheri Y, Zheng J, Moskowitz C, Udo K, Eastham J, Hricak H 2011 Diffusion-weighted endorectal MR imaging at 3 T for prostate cancer: tumor detection and assessment of aggressiveness. Radiology **259:**775–784.
18. Itou Y, Nakanishi K, Narumi Y, Nishizawa Y, Tsukuma H 2011 Clinical utility of apparent diffusion coefficient (ADC) values in patients with prostate cancer: can ADC values contribute to assess the aggressiveness of prostate cancer? J Magn Reson Imaging **33:**167–172.
19. Curvo-Semedo L, Lambregts DM, Maas M, Beets GL, Caseiro-Alves F, Beets-Tan RG 2012 Diffusion-weighted MRI in rectal cancer: apparent diffusion coefficient as a potential noninvasive marker of tumor aggressiveness. J Magn Reson Imaging **35:**1365–1371.
20. Bozgeyik Z, Coskun S, Dagli AF, Ozkan Y, Sahpaz F, Ogur E 2009 Diffusion-weighted MR imaging of thyroid nodules. Neuroradiology **51:**193–198.
21. Erdem G, Erdem T, Muammer H, Mutlu DY, Firat AK, Sahin I, Alkan A 2010 Diffusion-weighted images differentiate benign from malignant thyroid nodules. J Magn Reson Imaging **31:**94–100.
22. Mutlu H, Sivrioglu AK, Sonmez G, Velioglu M, Sildiroglu HO, Basekim CC, Kizilkaya E 2012 Role of apparent diffusion coefficient values and diffusion-weighted magnetic resonance imaging in differentiation between benign and malignant thyroid nodules. Clin Imaging **36:**1–7.

23. Nakahira M, Saito N, Murata SI, Sugasawa M, Shimamura Y, Morita K, Takajyo F, Omura G, Matsumura S 2011 Quantitative diffusion-weighted magnetic resonance imaging as a powerful adjunct to fine needle aspiration cytology for assessment of thyroid nodules. Am J Otolaryngol **33:**408–416.
24. Razek AA, Sadek AG, Kombar OR, Elmahdy TE, Nada N 2008 Role of apparent diffusion coefficient values in differentiation between malignant and benign solitary thyroid nodules. AJNR Am J Neuroradiol **29:**563–568.
25. Schueller-Weidekamm C, Kaserer K, Schueller G, Scheuba C, Ringl H, Weber M, Czerny C, Herneth AM 2009 Can quantitative diffusion-weighted MR imaging differentiate benign and malignant cold thyroid nodules? Initial results in 25 patients. AJNR Am J Neuroradiol **30:**417–422.
26. Schueller-Weidekamm C, Schueller G, Kaserer K, Scheuba C, Ringl H, Weber M, Czerny C, Herneth AM 2010 Diagnostic value of sonography, ultrasound-guided fine-needle aspiration cytology, and diffusion-weighted MRI in the characterization of cold thyroid nodules. Eur J Radiol **73:**538–544.
27. Tezuka M, Murata Y, Ishida R, Ohashi I, Hirata Y, Shibuya H 2003 MR imaging of the thyroid: correlation between apparent diffusion coefficient and thyroid gland scintigraphy. J Magn Reson Imaging **17:**163–169.
28. Prah DE, Paulson ES, Nencka AS, Schmainda KM 2010 A simple method for rectified noise floor suppression: phase-corrected real data reconstruction with application to diffusion-weighted imaging. Magn Reson Med **64:**418–429.
29. Raunig DL, McShane LM, Pennello G, Gatsonis C, Carson PL, Voyvodic JT, Wahl RL, Kurland BF, Schwarz AJ, Gonen M, Zahlmann G, Kondratovich M, O'Donnell K, Petrick N, Cole PE, Garra B, Sullivan DC, Group QTPW 2014 Quantitative imaging biomarkers: a review of statistical methods for technical performance assessment. Stat Methods Med Res **24:**27–67.
30. Kessler LG, Barnhart HX, Buckler AJ, Choudhury KR, Kondratovich MV, Toledano A, Guimaraes AR, Filice R, Zhang Z, Sullivan DC, Group QTW 2014 The emerging science of quantitative imaging biomarkers terminology and definitions for scientific studies and regulatory submissions. Stat Methods Medl Res **24:**9–26.
31. Ganly I, Ibrahimpasic T, Rivera M, Nixon I, Palmer F, Patel SG, Tuttle RM, Shah JP, Ghossein R 2014 Prognostic implications of papillary thyroid carcinoma with tall-cell features. Thyroid **24:**662–670.
32. Ghossein R, Ganly I, Biagini A, Robenshtok E, Rivera M, Tuttle RM 2014 Prognostic factors in papillary microcarcinoma with emphasis on histologic subtyping: a clinicopathologic study of 148 cases. Thyroid **24:**245–253.
33. Chenevert TL, Galban CJ, Ivancevic MK, Rohrer SE, Londy FJ, Kwee TC, Meyer CR, Johnson TD, Rehemtulla A, Ross BD 2011 Diffusion coefficient measurement using a temperature-controlled fluid for quality control in multicenter studies. J Magn Reson Imaging **34:**983–987.
34. Malyarenko D, Galban CJ, Londy FJ, Meyer CR, Johnson TD, Rehemtulla A, Ross BD, Chenevert TL 2013 Multi-system repeatability and reproducibility of apparent diffusion coefficient measurement using an ice-water phantom. J Magn Reson Imaging **37:**1238–1246.
35. Hu A, Clark J, Payne RJ, Eski S, Walfish PG, Freeman JL 2007 Extrathyroidal extension in well-differentiated thyroid cancer: macroscopic vs microscopic as a predictor of outcome. Arch Otolaryngol Head Neck Surg **133:**644–649.
36. Jukkola A, Bloigu R, Ebeling T, Salmela P, Blanco G 2004 Prognostic factors in differentiated thyroid carcinomas and their implications for current staging classifications. Endocr Relat Cancer **11:**571–579.
37. Cushing SL, Palme CE, Audet N, Eski S, Walfish PG, Freeman JL 2004 Prognostic factors in well-differentiated thyroid carcinoma. Laryngoscope **114:**2110–2115.
38. Shaha AR 2007 TNM classification of thyroid carcinoma. World J Surg **31:**879–887.
39. Hay ID, Bergstralh EJ, Goellner JR, Ebersold JR, Grant CS 1993 Predicting outcome in papillary thyroid carcinoma: development of a reliable prognostic scoring system in a cohort of 1779 patients surgically treated at one institution during 1940 through 1989. Surgery **114:**1050–1057; discussion 1057–1058.
40. Cady B, Rossi R 1988 An expanded view of risk-group definition in differentiated thyroid carcinoma. Surgery **104:** 947–953.
41. Hay ID, Grant CS, Taylor WF, McConahey WM 1987 Ipsilateral lobectomy versus bilateral lobar resection in papillary thyroid carcinoma: a retrospective analysis of surgical outcome using a novel prognostic scoring system. Surgery **102:**1088–1095.
42. Padhani AR, Koh DM 2011 Diffusion MR imaging for monitoring of treatment response. Magn Reson Imaging Clin N Am **19:**181–209.
43. Lawrence EM, Gallagher FA, Barrett T, Warren AY, Priest AN, Goldman D, Sala E, Gnanapragasam VJ 2014 Preoperative 3-T diffusion-weighted MRI for the qualitative and quantitative assessment of extracapsular extension in patients with intermediate- or high-risk prostate cancer. AJR Am J Roentgenol **203:**W280–286.
44. Chong Y, Kim CK, Park SY, Park BK, Kwon GY, Park JJ 2014 Value of diffusion-weighted imaging at 3 T for prediction of extracapsular extension in patients with prostate cancer: a preliminary study. AJR Am J Roentgenol **202:** 772–777.
45. Wang J, Takashima S, Takayama F, Kawakami S, Saito A, Matsushita T, Momose M, Ishiyama T 2001 Head and neck lesions: characterization with diffusion-weighted echoplanar MR imaging. Radiology **220:**621–630.
46. Koh DM, Collins DJ 2007 Diffusion-weighted MRI in the body: applications and challenges in oncology. AJR Am J Roentgenol **188:**1622–1635.
47. Maeda M, Kato H, Sakuma H, Maier SE, Takeda K 2005 Usefulness of the apparent diffusion coefficient in line scan diffusion-weighted imaging for distinguishing between squamous cell carcinomas and malignant lymphomas of the head and neck. AJNR Am J Neuroradiol **26:**1186–1192.

Address correspondence to:
R. Michael Tuttle, MD, and Amita Shukla-Dave, PhD
Department of Medicine; Departments of Medical Physics and Radiology
Memorial Sloan-Kettering Cancer Center
1275 York Avenue
New York, NY 10065

E-mail: tuttlem@mskcc.org; davea@mskcc.org